Simulations of the Titration of Linear Polyelectrolytes with Explicit Simple Ions: Comparisons with Screened Coulomb Models and Experiments

Magnus Ullner*,† and Clifford E. Woodward

School of Chemistry, University College, University of New South Wales, Australian Defence Force Academy, Canberra ACT 2600, Australia

Received June 30, 1999; Revised Manuscript Received March 27, 2000

ABSTRACT: Monte Carlo simulations of linear, weak polyacids and explicit simple ions have been performed in a spherical cell model to study the shift in the apparent dissociation constant. The simulations are performed in a canonical ensemble with the apparent dissociation constant calculated in a procedure based on Widom's particle-insertion method. The effects of model parameters are discussed, for example, the influence of various distances of closest approach, and the results are compared to experiments as well as simulations with effective pair-potentials between monomers, both the screened Coulomb potential and an extended version that takes into account a distance of closest approach between monomers and simple ions. Results of the latter potential are also compared to the experimental data, which are from poly(acrylic acid), poly-D,L-glutamic acid and carboxymethyl cellulose.

Introduction

A titrating polyelectrolyte is basically a large number of titrating sites collected into one molecule, for example, a polyacid or a polybase. Because of the proximity of the sites, they will interact, and the acid−base properties will be markedly different from a system where the same titrating sites are distributed on individual molecules, i.e., in corresponding monoacids and monobases. For example, if we have a polyacid and raise the pH, there will be a tendency for the sites to be increasingly deprotonated, but that also means that the total amount of charge will increase and the electrostatic interactions will oppose the deprotonation. The more highly charged the polyacid is, the harder it will be to increase the charge, and this will be reflected in an increasing apparent dissociation constant, which can be measured experimentally.

The apparent dissociation constant is defined as

$$\mathrm{p}K = \mathrm{pH} - \log\frac{\alpha}{1-\alpha} \qquad (1)$$

which looks like the equation for a monoacid, but for a monoacid pK would be constant and not increase with the degree of dissociation, α, as in the case of the polyacid. The difference in the acid−base properties of the polyacid and of a monoacid is expressed by

$$\Delta\mathrm{p}K = \mathrm{p}K - \mathrm{p}K_0 = \mathrm{pH} - \mathrm{p}K_0 - \log\frac{\alpha}{1-\alpha} \qquad (2)$$

where pK_0 is the dissociation constant of a monomer in the total absence of electrostatic interactions. The dissociation constant of a monomer in a neutral chain can also be used as a reference. In the latter case, there can still be electrostatic interactions between the monomer and simple ions in the surrounding solution.

There are two major effects that can influence ΔpK. When salt is added, the electrostatic interactions are reduced or "screened" and ΔpK will decrease for a given degree of dissociation. If the chain is flexible, it can expand as a response to the electrostatic repulsion, which also lowers ΔpK. We will be looking at both of these effects.

The properties of flexible, titrating polyelectrolytes have been studied by simulations of partially charged chains, where the charge was fixed,[1−7] and more directly in grand canonical simulations where the charge was allowed to fluctuate.[5,8−11] With one exception, ref 2, these studies treated the electrostatic interactions through an effective pair-potential between monomers only. In particular, any addition of salt was modeled through the screened Coulomb potential. This potential is a result of the Debye−Hückel approximation, which assumes a linear, additive electrostatic response.[12] It is only expected to be valid at low charge densities, because there is a nonlinear accumulation of countercharge at high charge densities. The extra amount of countercharge gives additional "screening" and the Debye−Hückel approximation should overestimate ΔpK at high charge densities.

Comparison with experiments has shown that the screened Coulomb potential gives titration curves that depend too strongly on the (implicit) salt concentration.[11] It is therefore of interest to take the simple ions into account explicitly. Simulations with flexible chains and explicit ions were first performed by Valleau for a fully charged chain in a spherical cell,[13] and Christos and Carnie have studied the structural properties of a partially ionized polyelectrolyte in a cubic box with periodic boundary conditions.[2] We are using simulations of a partially ionized polyelectrolyte with explicit ions to obtain its titration curve. Like Valleau,[13] we have used a cell model.[14−17]

The inclusion of explicit ions, both the counterions from the polyelectrolyte itself and any added salt, has two major effects. First, the cell-model results depend on the polyelectrolyte concentration, because the con-

* To whom correspondence should be addressed.
† Present address: Physical Chemistry 1, Center for Chemistry and Chemical Engineering, Lund University, P.O. Box 124, S-221 00 Lund, Sweden.

10.1021/ma991056k CCC: $19.00
Published on Web 08/25/2000

centration of the polyelectrolyte's own counterions and their screening effect also changes. Second, the explicit ions can give rise to various correlation effects that are not accounted for by the effective potential.

We will only briefly look at the concentration effects. We are more interested in the correlation effects and will therefore focus on systems with enough added salt to make the concentration effects minimal. What we want to investigate is how serious the neglect of the nonlinear electrostatic correlations is in the screened Coulomb model and if the explicit ions in the cell model improve the agreement with experiment.

From his simulations with explicit ions, Valleau concluded that "there is no reason to expect the screened Coulomb potential to have any utility in understanding the forces within polyions nor in predicting their conformational behavior".[13] He arrived at this conclusion by including the polyion charges in the calculated charge distributions, arguing that the polyion charges should contribute to the screening. This is not consistent with the way the screened Coulomb potential is normally used. When the interactions between all monomers are calculated using an effective potential, only species not considered explicitly should be included in the screening; i.e., the polyion charges should *not* be included.

By comparing ΔpK from simulations using the screened Coulomb potential with the results from the corresponding cell models, we can see how well the Debye−Hückel approximation describes the electrostatic interactions. The words "corresponding cell model" poses a minor problem, however. The screened Coulomb potential assumes that there is no distance of closest approach between a simple ion and a monomer, while such a parameter is a necessity when explicit ions are simulated. If the explicit ions were allowed to come arbitrarily close to a monomer, we would get infinite energies. While the screened Coulomb model is of interest, because it is the one that has been used previously, we are also making comparisons with an extended screened Coulomb potential,[18,20] which does include a monomer−ion distance of closest approach. This gives us a Debye−Hückel model that corresponds more closely to the cell model.

Comparisons between the normal screened Coulomb model and experiments have been published elsewhere.[11] We will therefore concentrate on the cell model and the extended screened Coulomb results in comparison to the same experimental data. The screened Coulomb potential was able to reproduce some of the features of the experimental titration curves, but not all. In particular, the salt dependence was too strong, as mentioned above. It is therefore of interest to see if the extended screened Coulomb model can yield a better fit, although it can be argued that this model is physically as questionable as the normal screened Coulomb potential and any improvement is just due to the fact that there is an extra fitting parameter. However, it highlights some of the general problems in comparisons between theoretical models and experimental data.

The paper is outlined as follows. We begin by describing the models used, followed by the statistical mechanics of polyacids, in particular expressions for calculating $pH - pK_0$ and ΔpK in the canonical ensemble. After a brief mentioning of the simulation algorithms, we move on to the results and discussion, which cover a comparison between a finite-chain expression and an infinite-chain approximation, the reference dissociation constant, screened Coulomb models vs the cell model, and simulation models vs experiments. We also give a brief summary of the effects of the model parameters on the titration curve before we conclude the paper. Expressions for calculating ΔpK of a finite chain in the canonical ensemble are derived in two appendices.

The number of parameters and symbols that we will be using is fairly large, and as a quick reference, Table 1 lists the most important ones.

Table 1. Frequently Used Symbols

b	bond length
N	number of monomers
n	number of charges
α	degree of dissociation
σ_{pp}	distance of closest approach between monomers
σ_{pi}	distance of closest approach between monomers and simple ions
σ_{ii}	distance of closest approach between simple ions
R_c	cell radius
c_p	monomer concentration
c_s	concentration of added salt
pK_0	dissociation constant of a monomer in the absence of electrostatic interactions (constant)
pK'_0	dissociation constant of a monomer in an uncharged (neutral) chain (varies with the concentration of simple ions)
pK	apparent dissociation constant
$\Delta pK = pK - pK_0$	shift in the apparent dissociation constant with pK_0 as reference
$\Delta pK' = pK - pK'_0$	shift in the apparent dissociation constant with pK'_0 as reference

Simulation Models

The Chain. The linear polyelectrolyte is modeled as a freely jointed chain of N monomers connected by rigid bonds. The bond length b represents an average distance between neighboring titrating sites. As a model of polyacids such as poly(acrylic acid), where the titrating groups sit at the ends of side chains, the bond length represents the average distance from the end of one side chain to the end of the next. With poly(acrylic acid) in mind, other simulation models have had a bond length corresponding to the monomer−monomer distance along the backbone,[1,2,6,7] but this is expected to give a charge−charge separation that is too short, which has been confirmed by comparison with experimental titration curves (see also the results here).[11]

Many other models for flexible titrating polyelectrolytes, lattice models[3,4,9,7] as well as off-lattice models,[1,2,5,6,8] have a fixed bond angle. Our model does not, because it is not clear what the value of the angle should be, especially not in our case where the chain does not represent the backbone.

To make the chain self-avoiding even in the absence of charge, the monomers are treated as hard spheres with respect to each other. The distance of closest approach between monomers is denoted σ_{pp}.

Since we will be looking at polyacids, each monomer can be neutral (protonated) or carry one negative unit of elementary charge (deprotonated). The charges can move freely along the chain.

Cell Model. In the cell model simulations the degree of dissociation will be fixed at $\alpha = n/N$, with n being the number of charges on the chain; i.e., n sites are deprotonated.

A monomer at the middle of the chain (position $N/2$) is fixed at the center of a confining spherical cell (radius R_c), whose volume corresponds to a given polyelectrolyte

concentration, expressed as the monomer concentration c_p. In all cases considered, the polyelectrolyte concentrations are low enough to avoid any conformational bias due to contacts with the wall of the cell. There are also n monovalent counterions in the cell as well as ion pairs corresponding to a 1:1 salt of concentration c_s.

Like the monomers, the simple ions are hard spheres and the implicit solvent (water) is treated as a dielectric continuum with a dielectric constant ϵ_r. The total interaction energy is composed of an electrostatic part and a hard-sphere part

$$U = U^{el} + U^{hs} = \sum_{i<j} \frac{z_i z_j e^2}{4\pi\epsilon_r\epsilon_0 r_{ij}} + \sum_{i<j} u_{ij}^{hs}(r_{ij}) \qquad (3)$$

where the sums extend over all pairs of monomers and ions in the cell. z_i is the valency of site i ($z_i = -1$, 0, or 1). e is the elementary charge, ϵ_0 the permittivity of vacuum, r_{ij} the distance between sites i and j and

$$u_{ij}^{hs}(r) = \begin{cases} \infty & r < \sigma_{ij} \\ 0 & r \geq \sigma_{ij} \end{cases} \qquad (4)$$

is the hard-sphere pair interaction with σ_{ij} being the distance of closest approach. The simulations are performed at a temperature $T = 298$ K and with $\epsilon_r = 78.3$, which gives a Bjerrum length $l_B = e^2/(4\pi\epsilon_r\epsilon_0 k_B T)$ of about 7.16 Å. k_B is Boltzmann's constant. The distance of closest approach between ions, denoted σ_{ii}, is 4 Å.[13,2]

There are no interactions beyond the cell, and correlations between the cells that implicitly make up the total (macroscopic) solution are neglected in these simulations. Simulations comparing a cell model and an isotropic solution of spherical micelles have shown that the cell model is a good approximation at low polyelectrolyte concentrations.[20]

Screened Coulomb Models. In the Debye−Hückel approximation,[12] the screening of the simple ions is treated implicitly with the following (screened Coulomb) potential

$$u_{ij}^{sc}(r_{ij}) = \frac{z_i z_j e^2}{4\pi\epsilon_r\epsilon_0} \frac{e^{-\kappa r_{ij}}}{r_{ij}} \qquad (5)$$

In the presence of a 1:1 salt, the Debye screening parameter is given by

$$\kappa^2 = 8\pi l_B N_A c_s \qquad (6)$$

where c_s is the concentration of added salt and N_A is Avogadro's number. This assumes an infinitely dilute polyelectrolyte solution, as the counterions originating from the polyelectrolyte do not contribute to κ. A simple way to include a dependence on the polyelectrolyte concentration would be to include the (monovalent) counterions in the screening parameter, i.e., to redefine it as $\kappa_{eff}^2 = 4\pi l_B N_A(\alpha c_p + 2c_s)$, where $c_s = 0$ in the salt-free case. However, in the systems we study here, the effect of doing this is small. Thus, the counterion contribution to κ will generally be ignored.

The total interaction energy (corresponding to eq 3) is

$$U = U^{el} + U^{hs} = \sum_{i<j} u_{ij}^{sc}(r_{ij}) + \sum_{i<j} u_{ij}^{hs}(r_{ij}) \qquad (7)$$

where the sums only extend over pairs of monomers.

In the screened Coulomb potential, the simple ions and monomers are treated as point charges. It is possible to extend the screened Coulomb potential to account for ion exclusion around the monomers,[18,19]

$$u_{ij}^{esc}(r_{ij}) = \frac{z_i z_j e^2}{4\pi\epsilon_r\epsilon_0} \frac{e^{2\kappa\sigma_{pi}}}{(1+\kappa\sigma_{pi})^2} \frac{e^{-\kappa r_{ij}}}{r_{ij}} \qquad (8)$$

where σ_{pi} is the distance of closest approach between a monomer and an (implicit) ion.

Statistical Mechanics

Ensembles. In the case of a titrating polyelectrolyte, an equilibrium is established between all dissociated forms of the polyelectrolyte at a given pH. This is directly taken into account in a grand canonical ensemble, whereby the charge on a chain can fluctuate while the proton chemical potential is held fixed. The grand canonical can therefore be called the natural ensemble for a titrating system.

We shall treat the charged (deprotonated) sites as the fluctuating species. The (bulk) chemical potential of these "particles" is related to the pH via[8,21]

$$\mu = k_B T \ln 10\ (\mathrm{pH} - \mathrm{p}K_0) \qquad (9)$$

The reference, pK_0, is the dissociation constant of a monomer in the absence of electrostatic interactions.

The grand partition function is

$$\Xi = \sum_{n=0}^{N} e^{\beta\mu n} \frac{1}{n!} Z_n \qquad (10)$$

with

$$Z_n = \begin{bmatrix} 1 & n = 0 \\ \sum_{\{\boldsymbol{x}^n\}} e^{-\beta U(\boldsymbol{x}^n)} & n > 0 \end{bmatrix} \qquad (11)$$

and $\beta = 1/k_B T$. $\boldsymbol{x}^n$ is an n-dimensional vector that represents the positions of the n charges. Each element x_i has a value that corresponds to a titrating site, i.e., a value from the set $\{1, 2, ..., N\}$, with N being the number of sites or monomers in our model. The summation in the configuration sum, Z_n, runs over all possible combinations of coordinates for the n charges. The total energy $U(\boldsymbol{x}^n)$ is the potential of mean force obtained by averaging over the coordinates for the simple ions and the conformations of the polyelectrolyte at a fixed configuration $\boldsymbol{x}^n$ of charges on the chain. We will call the collection of states with a given n a dissociation state.

In the grand canonical ensemble, the degree of dissociation, α, is obtained as an average (the equilibrium value)

$$\langle\alpha\rangle = \left\langle \frac{n}{N} \right\rangle = \frac{1}{N\Xi} \sum_{n=1}^{N} e^{\beta\mu n} \frac{n}{n!} \sum_{\{\boldsymbol{x}^n\}} e^{-\beta U(\boldsymbol{x}^n)} \qquad (12)$$

In the thermodynamic limit of the polyelectrolyte ($N \to \infty$ and $n \to \infty$ while $0 < \alpha = n/N < 1$ is fixed), the distribution of dissociation states becomes narrow and one dissociation state will dominate the sum in eq 10. That state will satisfy the equation

$$\beta\mu = -\frac{\partial}{\partial n}\ln Q_n \tag{13}$$

where

$$Q_n = \frac{Z_n}{n!} \tag{14}$$

Q_n is the partition function for the chain in a given dissociation state n.

Equation 13 states the usual equilibrium condition that the chemical potential of the charged species on the chain is equal to that of the bulk. In the canonical ensemble (fixed n), this condition is determined by calculating μ (or pH − pK_0) from eq 13. In the grand canonical ensemble (fixed μ) the average dissociation state is determined instead (cf. eq 12). The canonical ensemble and grand canonical results should be equivalent in the thermodynamic limit.

Simulations in the grand canonical ensemble are straightforward when the effect of salt is accounted for by using an effective monomer−monomer potential, for example, the screened Coulomb potential. Consequently, we have used this ensemble for the screened Coulomb models, as in previous simulations.[5,8−11]

However, if the grand canonical ensemble is used when explicit ions are simulated in a finite cell, the number of simple ions in the cell need to fluctuate to balance the fluctuations of the charge on the chain. Thus, the effective chemical potential of the chain charges will be mixed with that of the simple ions and this must be accounted for in order to obtain the corresponding pH − pK_0.[22] We have instead chosen to perform the explicit salt simulations in the canonical ensemble, where the numbers of all particles, chain charges as well as simple ions, are constant. Thus, we can avoid the correction for the salt contribution. This, together with a simpler set of Monte Carlo moves, makes the canonical ensemble simulations more convenient than those in the grand canonical ensemble.

Experimental polyelectrolytes are usually very long. If a chain is very much longer than the range of the intramolecular electrostatic interactions, screened by the simple ions, then the chain ends should have little effect on μ. To compare with experiments, therefore, we need to estimate ΔpK for an infinite chain. The canonical ensemble is actually well suited for this as will be discussed in the next section.

A proper treatment of the *finite* chain is complicated in the canonical ensemble. For completeness, we will also discuss this case in a subsequent section.

Local Expressions and the Infinite-Chain Limit. In the limit of an infinite chain, all monomers are equivalent. A polyelectrolyte may be considered to have reached the infinite-chain limit if it is much longer than the electrostatic correlation length (screening length). Under these conditions, most monomers, interacting with their local environment, do not feel the influence of the ends. Charge tends to accumulate at the ends of finite chains, where the electrostatic repulsion is reduced relative to the center. If the number of monomers is large enough, the average degree of dissociation is unaffected by any accumulation of charge toward the ends. Real polyelectrolytes are often long enough for these conditions to apply (provided that some salt has been added).

For the chain lengths used in this study, the amount of excess charge around the terminal monomers is a significant fraction of the average degree of dissociation. This notwithstanding, the local degree of dissociation is reasonably constant in the central portions of the chain. This value is slightly lower than the overall α.[7,10] This implies that the monomers at the center of the finite chain exist in an environment that approximates that of an infinite chain with an average α equal to the lower, local value. We will therefore approximate the infinite-chain limit by averaging the local ΔpK and α over monomers in the central part of the chain. To be specific, we will average over the four central monomers.

A similar inifinite chain approximation can also be used in the grand canonical ensemble. In this case, the local ΔpK is obtained directly from eq 2 by using the centrally averaged values of α.

In canonical ensemble simulations, the dissociation state, n, is chosen a priori and pH − pK_0 is calculated from the chemical potential. The chemical potential can be obtained by using Widom's particle insertion method.[23] For our purposes it is useful to use a local version of Widom's method. The resulting expression for pH − pK_0 is

$$\mathrm{pH} - \mathrm{p}K_0 = -\log\langle e^{-\beta\Delta U_+(x',\boldsymbol{x}^n)}\rangle_n + \log\langle\alpha(x')\rangle_{n+1} \tag{15}$$

$\Delta U_+(x',\boldsymbol{x}^n)$ is the change in energy when a charge is added to position x' with n charges at positions $\boldsymbol{x}^n$. Note that $\Delta U_+(x',\boldsymbol{x}^n)$ is infinite when a charge is already present at x'. The angular brackets $\langle\ldots\rangle_n$ denote the ensemble average for the indicated dissociation state and $\langle\alpha(x')\rangle_{n+1}$ is the local degree of ionization at site x' in the next higher dissociation state, $n + 1$. The average in the first term on the right-hand side, containing the change in energy, is calculated via a charging process,[24] which corrects for the implicit charge nonneutrality (for further details see the end of appendix A). At equilibrium the right-hand side of eq 15 is invariant to the site of insertion, x'. A similar expression is obtained using Widom's method to instead *remove* a charged particle from the chain, which is formally equivalent to inserting a proton. This gives

$$\mathrm{pH} - \mathrm{p}K_0 = \log\langle e^{-\beta\Delta U_-(x',\boldsymbol{x}^n)}\rangle_n - \log\langle 1 - \alpha(x')\rangle_{n-1} \tag{16}$$

$\Delta U_-(x',\boldsymbol{x}^n)$ is the change in energy when a charge is removed at position x', and it is infinite if there is no charge to remove. In the thermodynamic limit, both eqs 15 and 16 will give the same result. In this limit

$$\langle\alpha(x')\rangle_{n\pm1} \approx \langle\alpha(x')\rangle_n \tag{17}$$

Because of finite size effects there will be a small discrepancy between these expressions. For this reason we will use the average of eqs 15 and 16, together with eq 17, in eq 2, to calculate a local apparent dissociation constant

$$\Delta\mathrm{p}K(x') = \frac{1}{2}\left[\log\langle e^{-\beta\Delta U_-(x',\boldsymbol{x}^n)}\rangle_n - \log\langle e^{-\beta\Delta U_+(x',\boldsymbol{x}^n)}\rangle_n - \log\frac{\langle\alpha(x')\rangle_n}{1 - \langle\alpha(x')\rangle_n}\right] \tag{18}$$

As stated earlier, the infinite-chain approximation corresponds to averaging Δp$K(x')$ and $\langle\alpha(x')\rangle_n$ over those x' corresponding to the central four monomers. There is a potential computational advantage in the canonical

ensemble as only those sites need to be probed with Widom's method.

Finite Chains. In some cases, it may be of interest to consider the behavior of chains of finite length. For example, one may wish to investigate the effect of molecular weight on polyelectrolyte titration. Grand canonical simulations are the most appropriate for this problem. This is because, for a chain of finite length, dissociation states other than the most probable may have significant weight and these states are sampled properly in grand canonical simulations.

However, it is possible to make reasonably accurate predictions for finite-chain behavior using the canonical ensemble. An expression for $\mathrm{pH} - \mathrm{p}K_0$ for finite chain is obtained by random insertions of charges

$$\mathrm{pH} - \mathrm{p}K_0 = -\log \frac{1}{N}\sum_{x'=1}^{N}\langle \mathrm{e}^{-\beta\Delta U_+(x',\boldsymbol{x}^n)}\rangle_n + \log\frac{n+1}{N} \tag{19}$$

a similar equation based on charge removal is given by

$$\mathrm{pH} - \mathrm{p}K_0 = \log \frac{1}{N}\sum_{x'=1}^{N}\langle \mathrm{e}^{-\beta\Delta U_-(x',\boldsymbol{x}^n)}\rangle_n - \log\frac{N-n+1}{N} \tag{20}$$

As a first approximation, we can calculate $\mathrm{pH} - \mathrm{p}K_0$ as the average of eqs 19 and 20. In a canonical simulation with n charges, this corresponds to giving equal weights to the dissociation states on either side of this value, i.e., $n - 1$ and $n + 1$ (see appendix A). This method is accurate if the weight distribution is symmetric or if other dissociation states are of negligible weight. These are reasonable approximations over most of the range of α. However, when there are only one or two charged or uncharged monomers, the weight distribution is not symmetric. This is because of the truncations at $n = 0$ and $n = N$, respectively. As a result, $\mathrm{pH} - \mathrm{p}K_0$ calculated from the average of eqs 19 and 20 may differ significantly from the result of simulating in the grand canonical ensemble. In appendix B, we detail a mean-field correction procedure that approximates the distribution of dissociation states, calculated from a single canonical ensemble simulation.

Reference Dissociation Constant. In cell model simulations, the reference dissociation constant, $\mathrm{p}K_0$, is made independent of ionic strength by defining it to be the dissociation constant of a monomer in an uncharged polyelectrolyte (neutral chain) at infinite dilution in a salt-free solution. Thus, a finite salt concentration will give a contribution to $\Delta\mathrm{p}K$ even when there are no electrostatic intramolecular interactions (neutral chain).

When the screened Coulomb potential is used to model interactions between monomers, the salt ions are treated implicitly. It is then natural to include in the reference, the direct interaction between a charged monomer and the (implicit) salt at the specified concentration. We will denote this reference as $\mathrm{p}K'_0$.

To compare the cell-model simulations with the screened Coulomb results, we have to shift one of the sets of titration curves. There are two possibilities. We can be consistent with the Debye−Hückel approximation and use the corresponding self-energy of a monovalent charge $-\kappa l_B/2\ (1 + \kappa\sigma_{pi})$, i.e., shift the screened Coulomb results to $\Delta\mathrm{p}K = \Delta\mathrm{p}K' - \kappa l_B/2 \ln 10(1 + \kappa\sigma_{pi})$, where $\Delta\mathrm{p}K' = \mathrm{p}K - \mathrm{p}K'_0$.

The other alternative is to use the contribution from the simple ions to the charging of a single monomer in a neutral chain, which can be calculated from the charge-removal process in a cell-model simulation of a chain with just one charge. Averaging over all monomers, this gives

$$\Delta\mathrm{p}K' = \Delta\mathrm{p}K - \frac{1}{N}\sum_{x'=1}^{N}[\log\langle \mathrm{e}^{-\beta\Delta U_-(x',x_1)}\rangle_1 - \log\langle\alpha(x')\rangle_1] \tag{21}$$

The Debye−Hückel approximation neglects ion−ion correlation and the two options give slightly different results (see Results and Discussion). It is therefore better to shift the cell-model results. That way all titration curves will begin at the origin.

Monte Carlo Simulations

All Monte Carlo simulations are performed with the traditional Metropolis algorithm[25] for a single chain. The cell-model simulations have been described in detail in ref 26. In that work, however, the polyelectrolyte charge was static. Here we will allow unit charges to move between monomers, but the total charge on the chain is still constant, as is the concentration of added salt (canonical ensemble with respect to all particles). The trial configurations are obtained by randomly picking occupied and unoccupied sites and exchanging the charge between them. The number of charge moves per chain-conformation move (cf. ref 26) is the smaller of $n/4 + 1$ and $(N - n)/4 + 1$.

Grand canonical ensemble simulations of the screened Coulomb model have also been described previously.[10,11]

Results and Discussion

Infinite-Chain Approximation and Finite-Chain Expression. Even with $N = 80$, the accumulation of charge at the ends lowers the average degree of dissociation in the central part of the chain by a small, but significant, amount. In our worst case, i.e., the salt-free case with $b = 3$ Å at extreme dilution ($c_p = 8 \times 10^{-12}$ M), the local α in the middle of the chain is about 90% of the total degree of dissociation. However, as discussed above, α is locally constant over a large part of the chain's interior, which is the basis for our infinite-chain approximation. Figure 1 shows the titration curves obtained via this approximation in the cell model. Also shown is the finite-chain result (see appendices A and B). It is clear that the infinite-chain approximation converges much more rapidly with N than does the finite-chain result. In fact, with the infinite-chain approximation, $N = 40$ is enough to reach the limiting value when the concentration of added (1:1) salt is 0.01 M and just $N = 20$ is enough for $c_s = 0.1$ M. We will use the 80-mer in our comparison with experiment, though it is clear that shorter chains could have been used.

Figure 2 shows that there is very little difference between the infinite-chain approximation and the finite-chain expression for $N = 80$. The difference becomes smaller as N increases and for $N = 160$, it is virtually gone, even in the salt-free case (with monomer concentration $c_p = 0.0098$ M).

Reference Dissociation Constant. Table 2 shows values of $\mathrm{p}K'_0 - \mathrm{p}K_0$ predicted by Debye−Hückel theory compared to the ones calculated in the cell model. In the Debye−Hückel approach treating everything as point charges, the relative error can be more than 100%.

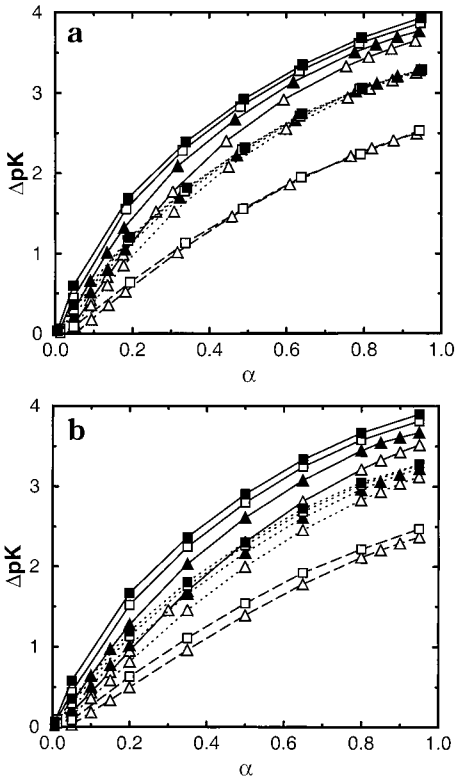

Figure 1. Effect on the titration curve from variations in the number of monomers for three concentrations of added salt: 0 (solid lines), 0.01 M (dotted lines), and 0.1 M (dashed lines). ΔpK has been calculated from (a) the infinite-chain approximation (average ΔpK and α from the four monomers at the center of the chain) and (b) the finite-chain expression (all monomers contributing). The numbers of monomers are 20 (open triangles), 40 (filled triangles), 80 (open squares), and 160 (filled squares) with $b = 3$ Å, $\sigma_{pp} = \sigma_{pi} = 4$ Å, and $c_p = 0.0098$ M.

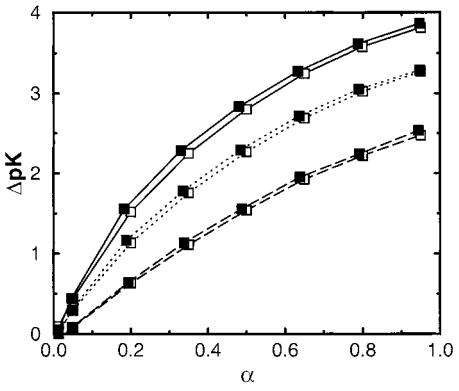

Figure 2. Comparison between the infinite-chain approximation (filled symbols) and the finite-chain expression (open symbols) for the chains with $N = 80$ also shown in Figure 1. The concentrations of added salt are 0 (solid lines), 0.01 M (dotted lines), and 0.1 M (dashed lines).

The result is improved significantly by taking into account a distance of closest approach between the ions and a monomer. There is still a relative error between 10% and 40%, due to the neglect of ion−ion correlations, but in absolute terms, the difference to the cell model is small, only up to 0.03 pK units.

A larger distance of closest approach for the ions to a monomer, σ_{pi}, reduces the (favorable) electrostatic interactions between the monomer and the ions. As a consequence, $|pK'_0 \neq pK_0|$ becomes smaller. In the cell model, ions can also be excluded by monomers other than the one that is titrating. The effects of this indirect exclusion may depend on the position of the titrating monomer along the chain, the total number of monomers and the bond length as well as the salt concentration. These effects are too weak to be observed at $c_s = 0.01$ M, but there are some trends at $c_s = 0.1$ M. The values of $|pK'_0 - pK_0|$ averaged over the four monomers in the middle of the chain are slightly smaller than the average over the four monomers closest to the ends (not shown). The difference is about a hundredth of a pK unit or less. This indicates that favorable electrostatic interactions between central monomers and simple ions are reduced by the excluding effects of other parts of the chain. The monomers at the ends are more accessible. This effect is also apparent in the results in Table 2. Indirect exclusion should be larger for a more compact structure, i.e., for a lower value of σ_{pp}. For $N = 20$, $pK'_0 - pK_0$ appears not to be significantly dependent on the distance of closest approach between the monomers, while that is indeed the case for $N = 80$ at $c_s = 0.1$ M. The smaller molecule is thus not large enough to affect the ion atmosphere of single monomers. Note that the values are more or less the same for the two chains when $\sigma_{pp} = 4$ Å, which means that the 80-mer is sufficiently expanded by the hard-sphere interactions to make the indirect exclusion effects small and local. We did not observe any bond length dependence, which further indicates that any local effects are too small to be detected.

Table 2. $pK'_0 - pK_0$ Predicted by Debye−Hückel Theory (DH) and Calculated in the Cell Model Simulations (MC)[a]

			DH		MC	
c_s/M	σ_{pp}/Å	σ_{pi}/Å	point	sphere	$N = 20$	$N = 80$
0.01	1	4	−0.051	−0.045	−0.041	−0.039
		7	−0.051	−0.042	−0.037	−0.035
	4	4	−0.051	−0.045	−0.042	−0.040
		7	−0.051	−0.042	−0.038	−0.035
0.1	1	4	−0.162	−0.114	−0.096	−0.090
		7	−0.162	−0.094	−0.075	−0.070
	4	4	−0.162	−0.114	−0.098	−0.098
		7	−0.162	−0.094	−0.076	−0.074

[a]The DH results are calculated with σ_{pi} both 0 (point) and as specified in the table (sphere). The MC results are averaged over all monomers and given for two chain lengths with a bond length of 3 Å and a monomer concentration of 0.0098 M.

Comparison with Screened Coulomb Potentials. The dependence on the polyelectrolyte concentration in the cell model is greatest in a salt-free system, where the neutralizing counterions are alone with the chain. Although it has a limited value for the discussion of real systems, the salt-free case is of theoretical interest as a limiting case and can be used to test different models and ensembles.

Figure 3 shows the titration curves from grand canonical simulations where monomers interact with a bare Coulomb potential (no added salt). The infinite-chain approximation has been used. In fact, this approximation is not entirely valid as, in the absence of salt, end effects cannot be completely neglected. The results should therefore be interpreted as the average titration behavior for the central four monomers in a chain of given length. Also shown are the results of canonical ensemble simulations in a very large cell ($R_c = 10^5$ Å) with no added salt, but with explicit counterions. Again the infinite-chain approximation has been used. The agreement between the (screened) Coulomb

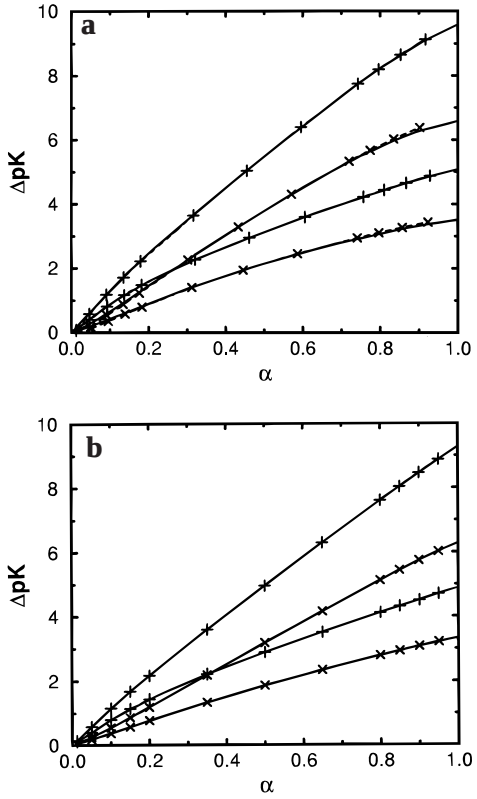

Figure 3. Comparison between grand canonical simulations (solid lines) and cell-model simulations (dashed lines with symbols) of hard-sphere chains ($\sigma_{pp} = 4$ Å) with $N = 20$ (×) and $N = 80$ (+) for (a) the infinite-chain approximation and (b) the finite-chain expression. The bond length for the upper curve in each set (given N) is 3 Å and 6 Å for the lower one. There is no added salt. The grand canonical case corresponds to an infinitely diluted chain (Coulombic interactions between monomers) and the monomer concentrations in the cell model with explicit counterions are 8×10^{-12} M and 3×10^{-11} M for the 20-mer and the 80-mer, respectively ($R_c = 10^5$ Å).

model and the cell model is very good. The small differences, in particular for $N = 20$ at low and high α, are due to fluctuations in the grand canonical ensemble simulations which are not present in the canonical ensemble simulations. For example, consider a chain with $N = 20$ and $\alpha = 0.05$. In the canonical ensemble, there is a single charge, which visits the different sites with equal probability. In the grand canonical ensemble, the total degree of dissociation of 0.05 is an average over different dissociation states. In particular, there are configurations with more than one charge on the chain contributing to the average and these charges are correlated. As a consequence, we get an uneven charge distribution with a higher probability of finding a charge at the ends than in the middle of the chain.[7,10] The charge−charge correlations also differ in the two ensembles when the number of *uncharged* monomers is close to 1 (on average), and these correlation differences affect ΔpK. In Figure 3b, we show the results for the same systems but where the canonical ensemble results are treated with the mean-field correction, outlined in appendix B. The agreement between the bare Coulomb (grand canonical) and cell model results (canonical) is excellent, which gives justification for our approximations.

Note that the excellent agreement between the models with and without explicit ions shows that there is no concentration independent accumulation of counterions around the polyelectrolyte as the often quoted Manning

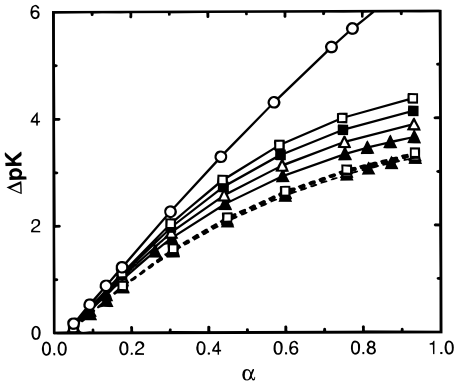

Figure 4. Effect on the titration curve (infinite-chain approximation) from variations in the polyelectrolyte concentration with no added salt (solid lines) and $c_s = 0.01$ M (dashed lines). Results are shown in both cases for monomer concentrations of 0.0098 M (filled triangles), 0.005 M (open triangles), 0.0024 M (filled squares), and 0.0012 M (open square). In addition for the salt-free case, results are plotted for $c_p = 8 \times 10^{-12}$ M (open circles), which is the same as the limiting titration curve at infinite dilution (cf. Figure 3). The chain parameters are $N = 20$, $b = 3$ Å, and $\sigma_{pp} = \sigma_{pi} = 4$ Å.

theory would predict.[27] The theory states that when the Manning parameter $\xi = \alpha l_B/b$ exceeds 1, counterions will "condense" to create an effective charge density ξ just less than one. Here we have have a value of ξ up to 2.3 ($\alpha = 0.95$, $b = 3$ Å). Still, the lack of Manning condensation is not at all surprising, since the theory was derived from a Debye−Hückel treatment of an infinite line charge and the effect is a consequence of a singularity in this treatment. In the cell model we have finite chains and the electrostatic energy is not large enough to compensate the very large entropy represented by having all the counterions spread out in a very large volume.

We checked if the agreement between the two models was due to sampling problems in the simulation. That this was *not* the case, was confirmed by starting the cell-model simulations with the counterions distributed randomly in the whole cell as well as with a distribution taken from a simulation with the smallest cell radius, i.e., with the counterions close to the polyacid. Given sufficient time for equilibration, both simulations gave the same result; i.e., Manning condensation did not occur.

Figure 4 indicates how ΔpK in the cell model (infinite-chain approximation) varies with the polyelectrolyte concentration for the salt-free case and with c_s comparable to c_p. The effect is minor in the latter case and we will focus on solutions where the concentration of added salt is as high as or larger than αc_p, to reduce the influence of the neutralizing counterions.

Values of ΔpK' from both cell-model and screened Coulomb simulations are plotted as functions of α in Figure 5. The infinite-chain approximation has been used. At $c_s = 0.01$ M, we get the expected result; i.e., the agreement is good at low degrees of dissociation (up to about $\alpha = 0.2$), and ΔpK for the screened Coulomb model is larger than the cell model results at higher α.

The hard-sphere interactions between the monomers are the same in the two models. This is necessary for the good agreement at low α, as hard-sphere interactions have a strong influence on the shape of the titration curve when the chain is not highly charged. With increasing size of the monomers, the chain is more expanded, which reduces the (unfavorable) intramo-

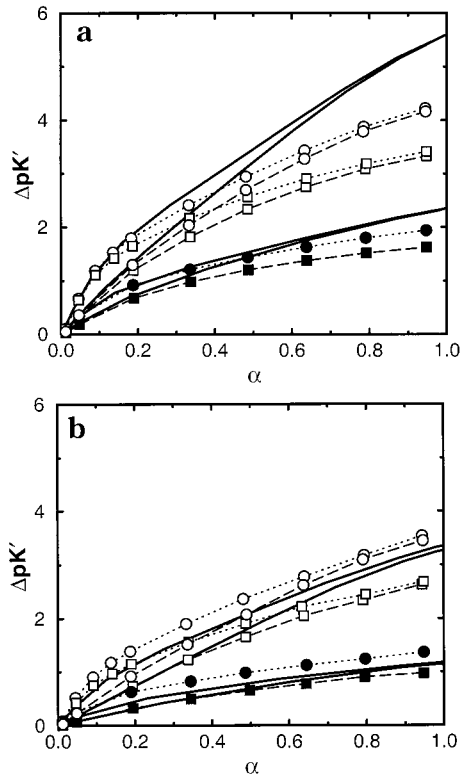

Figure 5. Comparison between screened Coulomb simulations (solid lines) and cell-model simulations (symbols) with (a) $c_s = 0.01$ M and (b) $c_s = 0.1$ M for $N = 80$. The bond lengths are 3 Å (upper pair of solid lines/open symbols) and 6 Å (lower pair/filled symbols). In each pair of screened Coulomb results, the distance of closest approach between monomers is $\sigma_{pp} = 1$ Å for the upper solid curve and 4 Å for the lower one. For the cell model, the hard-sphere parameters are $\sigma_{pp} = 1$ Å (dotted lines) and 4 Å (dashed lines) and $\sigma_{pi} = 4$ Å (squares) and 7 Å (circles). Monomer concentrations are 0.0098 M for $b = 3$ Å and 0.0049 M for $b = 6$ Å.

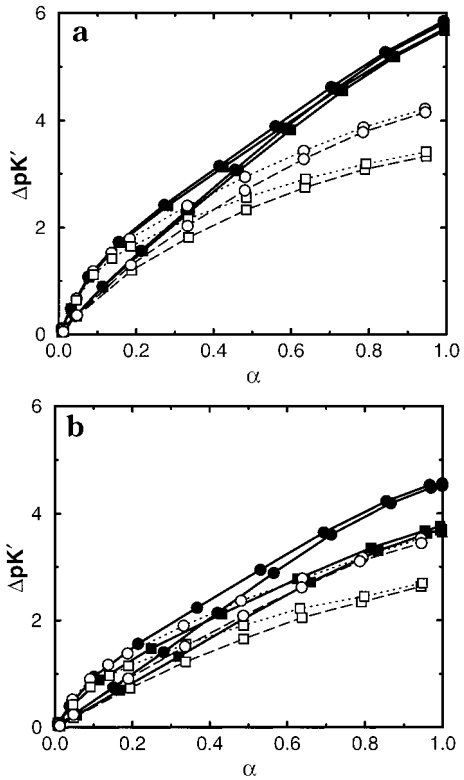

Figure 6. Comparison between simulations using an extended screened Coulomb potential, eq 8, (filled symbols, solid lines) and cell-model simulations (open symbols) with (a) $c_s = 0.01$ M and (b) $c_s = 0.1$ M for $N = 80$. The bond length is 3 Å with hard-sphere parameters $\sigma_{pp} = 1$ Å (upper curve in pairs of converging solid lines/dotted lines) and 4 Å (lower solid line in converging pairs/dashed lines) and $\sigma_{pi} = 4$ Å (squares) and 7 Å (circles). For the cell model $c_p = 0.0098$ M.

lecular electrostatic interactions and lowers $\Delta pK'$. At higher α, the hard-sphere interactions become less important, because the chain is expanded by the electrostatic interactions, and the screened Coulomb results with different monomer radii converge, if the other parameters are the same.

There is a similar convergence among the cell-model results, which also illustrates the effect of σ_{pi}. At higher α, the exclusion of simple ions by the monomers becomes increasingly important, because more ions are attracted by the chain. The larger the "ion-free zone" around the polymer, the less effective is the "screening". A larger value of σ_{pi} thus gives a larger $\Delta pK'$ at the higher degree of dissociation. In the cell model, titration curves for the same σ_{pi}, but different σ_{pp}, approach each other as α increases. In Figure 5, the curves for $b = 3$ Å with $(\sigma_{pp},\sigma_{pi}) = (1,4)$ and (4,7) cross over, which further illustrates the balance between the two hard-sphere parameters. Since the screened Coulomb potential treats the simple ions as point ions, it is unable to reproduce the splitting of titration curves due to σ_{pi} in the cell model.

The importance of σ_{pi} also increases with the amount of added salt, because more ions are excluded at a higher salt concentration. The cell model results with different values of σ_{pi} diverge at much lower values of α at $c_s = 0.1$ M than at $c_s = 0.01$ M. This also affects the comparison with the Debye−Hückel results. From Figure 5, we see that with $\sigma_{pi} = 4$ Å, the agreement between the two models looks better at $c_s = 0.1$ M than at $c_s = 0.01$ M. The models give similar results up to $\alpha = 0.3-0.4$ for $b = 3$ Å and even further for $b = 6$ Å. However, when $\sigma_{pi} = 7$ Å, there is generally no agreement even at very low degrees of dissociation. The effect of having $\sigma_{pi} = 7$ Å is even strong enough to make $\Delta pK'$ exceed the Debye−Hückel result at the higher salt concentration.

The extended screened Coulomb potential, eq 8, accounts for ion exclusion around the monomers in the Debye−Hückel treatment. The results for this model are shown in Figure 6. For $c_s = 0.01$ M, the modification does not have much effect, but at $c_s = 0.1$ M the agreement between the models is now reasonably good up to $\alpha = 0.2$ for both values of σ_{pi}. This suggests that the extended screened Coulomb model, as a linear theory, is more consistent and fails for α above 0.2. The absence of nonlinear effects means that the model overestimates $\Delta pK'$ at large α at any salt concentration. The nonlinear accumulation of counter charge at high α in the cell model makes ion-exclusion effects important even at lower salt concentrations. The cell model shows a splitting of the titration curves for different σ_{pi} that is of a similar size at both concentrations in Figure 6. The extended screened Coulomb potential also shows a splitting, but it is much larger at $c_s = 0.1$ M than at 0.01 M, and the Debye−Hückel results are still not meaningful at large degrees of dissociation.

Thus, the extended screened Coulomb potential gives a reliable improvement at low α, compared to the normal screened Coulomb model. The extended screened Coulomb potential is not valid at large α, but it is at

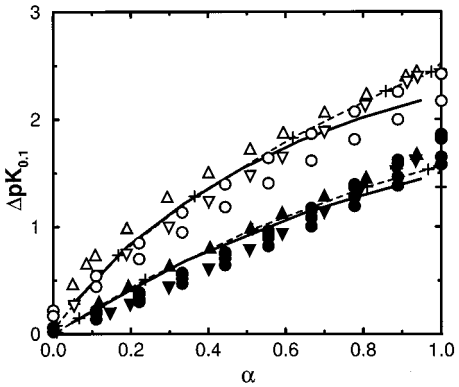

Figure 7. Comparison between cell-model simulations (solid lines), extended screened Coulomb (eq 8) simulations (dashed lines with plus signs) and experimental titration curves for poly(acrylic acid) (triangles and circles) at salt concentrations of 0.01 M (upper curves/open symbols) and 0.1 M (lower curves/filled symbols). The experimental data were obtained from Figure 1 of Kawaguchi and Nagasawa[29] for isotactic (triangles pointing up) and syndiotactic (triangles pointing down) poly(acrylic acid) and from the parameters for a fitted second-order polynomial tabulated by Mandel (circles).[28] In the latter case, we used the average of the four tabulated pK_0 values for c_s = 0.1 M as the reference, while for the other data, the reference was obtained by extrapolating graphically to $\alpha = 0$. The chain parameters in the cell-model simulations were $N = 80$, b = 4.5 Å, $\sigma_{pp} = 6$ Å, and $\sigma_{pi} = 4$ Å and the monomer concentration was 0.0098 M. In the extended screened Coulomb simulations, $N = 80$, $b = 6$ Å, $\sigma_{pp} = 4$ Å, and $\sigma_{pi} = 7$ Å. To mimic the ionic strength dependence of ΔpK at $\alpha = 0$, 0.04 pK units were added to the 0.01 M titration curve of the extended screened Coulomb results, which roughly corresponds to the shift seen in the cell model from 0.1 to 0.01 M at $\alpha = 0$ for $\sigma_{pp} = 4$ Å and $\sigma_{pi} = 7$ Å (cf. Table 2).

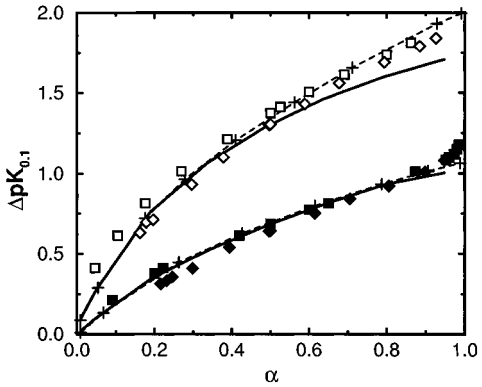

Figure 8. Comparison between cell-model simulations (solid lines), extended screened Coulomb (eq 8) simulations (dashed lines with plus signs) and experimental titration curves for poly-D,L-glutamic acid (squares), obtained from Figure 1 of Olander and Holtzer,[32] and carboxymethyl cellulose (diamonds), obtained from Figure 1 of Muroga et al.[33] The salt concentrations are 0.01 M (upper curves/open symbols) and 0.1 M (lower curves/filled symbols). The cell-model simulations were performed with $N = 80$, $b = 6$ Å, $\sigma_{pp} = \sigma_{pi} = 4$ Å, and c_p = 0.0049 M. The parameters for the extended screened Coulomb simulations were $N = 80$, $b = 7$ Å, $\sigma_{pp} = 3$ Å, and σ_{pi} = 5 Å and the resulting 0.01 M curve was shifted upward by 0.05 pK units, which roughly corresponds to the shift seen in the corresponding cell model.

least consistent with the neglect of nonlinear electrostatic effects, unlike the normal screened Coulomb potential, which shows a deceptively good agreement with the cell model for $\sigma_{pi} = 4$ Å at $c_s = 0.1$ M. The latter result is due to a cancellation of errors and shows that even good agreement can be doubtful.

Comparison with Experiments. To compare with experimental results, we need a reference value for ΔpK at $\alpha = 0$. Unfortunately, the ionic strength independent pK_0 for the experimental systems are not available. Instead, we have chosen to extrapolate the titration curves for both experiments and simulations, for c_s = 0.1 M and use this as our reference point in each case. In this way, the data is at least treated consistently. The resulting ΔpK will be denoted $\Delta pK_{0.1}$.

In addition to the reference, suitable values for the model parameters b, σ_{pp}, and σ_{pi} are also needed. We start by looking at the difference in ΔpK between the two salt concentrations ($c_s = 0.01$ and 0.1 M) for α close to 1. For the given set of parameters, the simulated difference appears to depend only on σ_{pi}. The experimental data we are comparing with all seem to have a similar salt dependence, which is close to the simulation results for $\sigma_{pi} = 4$ Å. The value of ΔpK at $\alpha \approx 1$ can then be fitted with the bond length, b, and the shape of the titration curve at low α can be adjusted with σ_{pp}.

Figure 7 shows a comparison with experimental measurements for poly(acrylic acid) and Figure 8 displays results for poly-D,L-glutamic acid and carboxymethyl cellulose, which have very similar behaviors. The chosen bond lengths, 4.5 and 6 Å, respectively, are reasonable. In our modeling, the bond represents an average distance between neighboring charges which are on side chains. In the case of poly(acrylic acid), for example, the monomer−monomer separation along the backbone of 2.5 Å, used in some simulations,[1,2,6,7] is obviously much too short as an effective bond length. An estimate based on standard bond lengths and bond angles gives a maximum charge distance of between 5 and 6 Å for poly(acrylic acid) (the lower value is more appropriate for the isotactic form), which compares well with the 4.5 Å of our model. For poly-D,L-glutamic acid, the maximum charge separation is 8−10 Å for nearest and next-nearest neighbors, to be compared with 6 Å in the model. In a previous study using the screened Coulomb potential,[11] reasonable agreement was obtained for the 0.01 M curve with bond lengths of 6 and 7 Å, respectively. The lower values given by the cell model reflects the nonlinear electrostatic response in this model, which lowers ΔpK compared to the Debye−Hückel approximation (cf. the previous section).

The fact that we get the same σ_{pi} in all our comparisons with experiments is consistent with the fact that all the experimental polyelectrolytes have carboxy groups as their titrating sites. It may not be meaningful to look too closely at the exact values of our parameters, but the values are reasonable and we believe that the cell model captures the essential features of titrating polyelectrolytes.

It is apparent, however, that the cell model titration curves seem to saturate too quickly at large α, compared to experiments. There is even a tendency to positive curvature in the experimental titration curves for c_s = 0.1 M, which is counter to the simulation results. This can be seen in in Figure 7 for syndiotactic poly(acrylic acid) and for carboxymethyl cellulose in Figure 8. The very sharp increase seen for poly-D,L-glutamic acid in the latter figure may be an artifact due to the large uncertainty of calculating $\log(\alpha/(1-\alpha))$ when α is close to 1. In the case of the second-order polynomial fit for poly(acrylic acid),[28] the titration curves seem to be shifted with respect to each other. This could be due to differences in the samples or a general uncertainty in the results. The curvature is negative when $c_s = 0.01$

M, but zero or positive for $c_s = 0.1$ M, which is consistent with the other experimental curves.

If we assume that the electrostatic interactions are treated realistically in the cell model, the results indicate that the polyelectrolyte model is too simple. One possibility is that it is too flexible and allows the chain to expand too much.

A stiffer polyelectrolyte model was simulated by fixing the bond angle at 109.5°, the value used by Christos and Carnie.[2] The titration curves are almost the same with or without the fixed angle (results not shown). As a matter of fact, a rigid rod has a nearly linear titration curve (zero curvature) in the Debye−Hückel description.[11] The nonlinear accumulation of countercharge around the polyacid, as occurs in the cell model, is expected to yield a negative curvature for this fixed conformation. Thus, even making the chain completely stiff would not reproduce the experimental trend toward a positive curvature at high salt concentrations.

There may also be an effect from the neutral atoms. They are neglected in our model, but could potentially exclude more ions, and thus reduce the "screening". The effect would be stronger at higher salt concentrations, both because of the larger number of excluded ions and because the chain would be less expanded, i.e., more compact. A more atomistically detailed model is needed to investigate this possibility.

The screened Coulomb results show less curvature at large α, which fits the experimental data better. However, it was concluded in a previous investigation that the screened Coulomb potential allows ΔpK to decrease too much compared to experiments when the salt concentration is increased.[11] With the extended screened Coulomb potential, eq 8, however, the difference between the titration curves for different salt concentrations can be reduced by increasing σ_{pi} (cf. Figures 5 and 6). This should allow a better fit of the experimental data. Nevertheless, we have already concluded that the Debye−Hückel approximation is not valid at large α, compared to the cell model. Thus, the validity of the model and the fit is highly questionable. However, it is still of theoretical interest.

Figure 7 shows the results of fitting the extended screened Coulomb potential. The model parameters for this 80-mer were $b = 6$ Å, $\sigma_{pp} = 4$ Å, and $\sigma_{pi} = 7$ Å. To mimic the ionic strength dependence of pK'_0, we have added 0.04 to the curve for $c_s = 0.01$ M. This is roughly the difference in $pK'_0 - pK_0$ between the results for $c_s = 0.01$ and 0.1 M in the cell model with the same σ_{pp} and σ_{pi} (cf. Table 2; $b = 6$ Å gives results similar to $b = 3$ Å). The extended screened Coulomb model gives very similar results to the cell model with $b = 4.5$ Å, $\sigma_{pp} = 6$ Å, and $\sigma_{pi} = \sigma_{ii} = 4$ Å up to $\alpha = 0.6$. Of course, both curves result from fitting to the same experimental data, but the agreement is remarkable nevertheless. At high α, the extended screened Coulomb results do not saturate as quickly as the cell model and therefore better fits the experimental data of at least Kawaguchi and Nagasawa.[29] A similar conclusion can be drawn from a comparison between the two types of models in Figure 8.

There is a pattern in the parameter values for the two types of simulation model. To fit the same experimental data, the cell model has a shorter bond length and smaller σ_{pi}, while σ_{pp} is larger than for the extended screened Coulomb model. This may be rationalized in terms of the general behavior of the two models. In the cell model, the nonlinear electrostatic effects lower ΔpK and the shorter bond compensates for this. The nonlinear effects are strongest at high α, however, and the larger σ_{pp} is needed to help lower ΔpK at low α and reduce the curvature in general. In the normal screened Coulomb potential, ΔpK is too strongly affected by an increase in the salt concentration, in particular at high α, which can be counteracted by the larger value of σ_{pi} in the extended potential.

We have confirmed that the infinite-chain approximation applied to the extended screened Coulomb results for 80-mers, gives exactly the same results as for the corresponding 320-mers, which is the chain length used in the previous study.[11] At these salt concentrations, the infinite-chain approximation and the finite-chain ΔpK, are the same in the case of $N = 320$, while there is a small difference at $c_s = 0.01$ M for $N = 80$.

We have seen that the extended screened Coulomb potential, can fit the experimental data better than the cell model, which is somewhat surprising. We interpret this as a cancellation of errors in the former. It may be argued that the good agreement for the extended screened Coulomb potential is physically meaningless and just a result of a having a large number of parameters to fit. Indeed, the more parameters, the better the fit should be. However, there is more to it than that as the number of parameters is exactly the same in the cell model.

Furthermore, we can argue that it is physically reasonable to have a monomer−ion exclusion parameter. We saw that it was actually needed to make the Debye−Hückel treatment agree with the cell model in a consistent manner at low α, where the Debye−Hückel approximation is expected to hold. In this case, it was not a fitting parameter. We knew the value of σ_{pi}. In the experimental case, we do not know the appropriate value a priori. However, the values needed to fit the experimental data seemed physically reasonable. Comparison with the cell model, shows that the extended screened Coulomb model is only valid up to about $\alpha = 0.2$. If the cell model simulations had not been done we could have mistakenly believed that the extended screened Coulomb model gives a physically valid description of reality. It is of interest, however, to ask if a model that reproduces one experimental property well, through a cancellation of errors, can yield good agreement for other properties as well. If that is the case, it may not matter if the actual parameter values have questionable physical significance. Thus, the (extended) screened Coulomb model may yet be of some use. We know, for instance, that the model gives qualitatively correct behavior for the electrostatic persistence length, in comparison with experiment.[30] To answer the question, we need a range of experimental data for different properties. We also need to investigate better simulation models, for example, an "all-atom" model. This is beyond the scope of the present paper, however.

Summary of the Effects of the Model Parameters on the Titration Curve

In the cell model, the polyelectrolyte model itself is specified by four parameters, b, σ_{pp}, σ_{pi}, and N, which have different effects on the titration curve. Here we list these effects as a quick reference, although many of them should be fairly obvious.

Qualitatively, ΔpK increases when (1) the bond length decreases, (2) the distance of closest approach between monomers decreases (mainly at low α), (3) the distance

of closest approach between monomers and simple ions increases (stronger effect at higher α and higher salt concentrations), and (4) the number of monomers increases (mainly for short chains and low salt concentrations).

In terms of concentrations, ΔpK will increase when (5) the concentration of added salt decreases and (6) the polyelectrolyte concentration decreases (mainly at low salt concentrations).

pK'_0 (the dissociation constant of a neutral polymer in the presence of simple ions) increases with (1) decreasing concentration of added salt, (2) decreasing concentration of the polyelectrolyte (mainly at low salt concentrations and $pK'_0 \to 0$ when $c_p \to 0$ for $c_s = 0$), and (3) increasing monomer−ion distance of closest approach.

At high concentrations of salt, pK'_0 may increase due to (weak) indirect effects when (4) the number of monomers increases and (5) the distance of closest approach between monomers decreases (more compact structures).

Conclusions

Because of an explicit treatment of ions, the cell model contains effects that are not directly obtainable from simulations using the screened Coulomb potential, in particular: (1) effects of the polyelectrolyte concentration, due to the neutralizing counterions (mainly at very low salt concentrations), (2) effects on pK'_0, due to ion−ion correlations (effects at $\alpha = 0$), and (3) nonlinear electrostatic effects, due to a nonlinear accumulation of countercharge around the polyelectrolyte (mainly at medium to large α).

In a salt-free system at very high (infinite) dilution, these effects are of no consequence and the screened Coulomb potential is in perfect agreement with the cell model, even at high charge densities. This shows that there is no "Manning condensation" in this case. This is not surprising, because the Manning theory was derived for an infinite chain,[27] while we have simulated short chains.

In the comparison with the screened Coulomb potential, we have focused on concentrations of added salt where the effect of the polyelectrolyte concentration is minimal. At $c_s = 0.01$ M, the effect of the monomer−ion exclusion in the cell model is small at low degrees of ionization and the screened Coulomb potential gives the same $\Delta pK'$ as the cell model up to about $\alpha = 0.2$. At $c_s = 0.1$ M, σ_{pi} is more important and the extended screened Coulomb potential is needed to give a consistent agreement. The extended screened Coulomb potential is valid up to around $\alpha = 0.2$ at both salt concentrations.

Although the nonlinear accumulation of charge around the polyelectrolyte is small at low α, there are still some ion−ion correlations, which can be seen in $pK'_0 - pK_0$. Once again the monomer−ion exclusion needs to be included in the Debye−Hückel treatment to improve the agreement at high salt concentrations. There is still a relative error between 10 and 40%, but it is almost insignificant in absolute terms, only up to 0.03 pK units.

At high degrees of dissociation the extended screened Coulomb potential always overestimates $\Delta pK'$, which is consistent with the neglect of a nonlinear accumulation of countercharge around the polyelectrolyte. The normal screened Coulomb potential is less consistent, because of its treatment of all charges as point ions.

The cell model gives a much better agreement with experiments than the screened Coulomb potential, but the inclusion of explicit ions also gives too much negative curvature at large α. In this respect, the extended screened Coulomb potential gives an even better fit, although we believe this to be due to a cancellation of errors and the physical significance is questionable. In a real system, we would expect nonlinear electrostatic effects. These are illustrated by the cell model, although the polyelectrolyte model itself may be too crude to optimally reproduce experimental data. Further investigations are needed to improve the model.

Acknowledgment. Without the kind permission to use the central LUNARC computer resource in Lund, Sweden, the time needed to obtain an extensive data set would have been even greater (several months more). This work was supported by the Swedish Natural Science Research Council.

Appendix A

In this appendix we derive an expression for $pH - pK_0$ by balancing the weights of the dissociation states $n + 1$ and $n - 1$. This is to be able to calculate $pH - pK_0$ for a finite chain from a single canonical simulation.

The value of $pH - pK_0$, or equivalently μ (see eq 9), that corresponds to our canonical simulation with n charges on the chain is the $pH - pK_0$ that would give the same degree of dissociation, $\alpha = n/N$, as the average (see eq 12) in a grand canonical simulation. If states $n - 1$, n, and $n + 1$ are the only states with a nonnegligible weight (a narrow and highly peaked distribution of weights) the average can be written as

$$\langle\alpha\rangle = \frac{1}{N}\frac{(n-1)W_{n-1} + nW_n + (n+1)W_{n+1}}{W_{n-1} + W_n + W_{n+1}} \quad (22)$$

The weights W_n are functions of μ (cf. eq 12) and if μ is chosen so that $W_{n-1} = W_{n+1}$, we will get $\langle\alpha\rangle = n/N$, as desired. The weight distribution is expected to become increasingly narrow as N increases.

$W_{n-1} = W_{n+1}$ will also hold, by definition, if the weight distribution is symmetric around state n, which is also a reasonable approximation for most values of n (but not when n is close to 1 or N, see appendix B).

The weights of the neighboring states relative to the simulated state, n, can be be obtained by a technique equivalent to Widom's method.[23] The logarithm of the weight ratio between state $n + 1$ and n is

$$\ln\frac{W_{n+1}}{W_n} = \beta\mu - \ln(n+1) + \ln\frac{Z_{n+1}}{Z_n} \quad (23)$$

with

$$\frac{Z_{n+1}}{Z_n} = \frac{1}{Z_n}\sum_{x'=1}^{N}\sum_{\{\boldsymbol{x}^n\}} e^{-\beta\Delta U_+(x',\boldsymbol{x}^n)} e^{-\beta U(\boldsymbol{x}^n)} = \sum_{x'=1}^{N}\langle e^{-\beta\Delta U_+(x',\boldsymbol{x}^n)}\rangle_n \quad (24)$$

For explanation of the symbols, see the text after eqs 11 and 15. The summation over x' on the far right-hand side means that a separate average should be calculated for each monomer. Similarly

$$\ln\frac{W_{n-1}}{W_n} = -\beta\mu + \ln n + \ln\frac{Z_{n-1}}{Z_n} \quad (25)$$

with

$$\frac{Z_{n-1}}{Z_n} = \frac{1}{n(N-n+1)Z_n}\sum_{x'=1}^{N}\sum_{x_n=1}^{N}\sum_{\{\boldsymbol{x}^{n-1}\}} \times e^{-\beta\Delta U_-(x',\boldsymbol{x}^n)} e^{-\beta\Delta U_+(x_n,\boldsymbol{x}^{n-1})} e^{-\beta U(\boldsymbol{x}^{n-1})} = \frac{1}{n(N-n+1)}\sum_{x'=1}^{N}\langle e^{-\beta\Delta U_-(x',\boldsymbol{x}^n)}\rangle_n \quad (26)$$

where the sum over the positions of the $n-1$ charges have been reexpressed using two extra summations that add a charge at x_n to the $n-1$ and subsequently subtract one of the n charges. This leads to an overcounting of states, which necessitates the renormalization. There are $N-n+1$ positions to put the extra charge and n ways to reduce the number again. The combined results of eqs 25 and 26 can also be obtained from eqs 23 and 24 with n representing the $N-n$ unoccupied sites.

With equal weights for the states $n+1$ and $n-1$, i.e., $W_{n+1}/W_{n-1} = 1$, we get

$$\mathrm{pH} - \mathrm{p}K_0 = \frac{\beta\mu}{\ln 10} = \frac{1}{2}\left[\log\sum_{x'=1}^{N}\langle e^{-\beta\Delta U_-(x',\boldsymbol{x}^n)}\rangle_n - \log\sum_{x'=1}^{N}\langle e^{-\beta\Delta U_+(x',\boldsymbol{x}^n)}\rangle_n + \log\frac{n+1}{N-n+1}\right] \quad (27)$$

The ensemble averages in eq 27 are for nonelectroneutral insertions and deletions of charges. This would not be a problem if we had an infinite (macroscopic) system that could respond to the perturbation, which would be infinitesimal with respect to the whole system. The simulated system is finite, however. To correct for this, the averages are not calculated directly, but via a charging process.[24] For the addition we have

$$\langle e^{-\beta\Delta U_+(x',\boldsymbol{x}^n)}\rangle_n = \langle 1-\alpha(x')\rangle_n \exp\left[-\int_0^1 d\lambda \frac{\langle\beta\Delta U_+(x',\boldsymbol{x}^n)e^{-\beta\lambda\Delta U_+(x',\boldsymbol{x}^n)}\rangle_n}{\langle e^{-\beta\lambda\Delta U_+(x',\boldsymbol{x}^n)}\rangle_n}\right] \quad (28)$$

Contributions to the integral, which is calculated from 11 points using the extended Simpson's rule,[31] only occur when position x' is unoccupied and the average probability of finding it so is $\langle 1-\alpha(x')\rangle_n$; i.e., the monomer has an average degree of dissociation $\langle\alpha(x')\rangle_n$. During the charging process, electroneutrality is maintained by rescaling the charges z_j on the simple ions with the factor $(1-\lambda z_\mathrm{p}/(z_j N_z))$, where $z_\mathrm{p} = -1$ is the monomer charge and N_z is the total number of simple ions. The average for deletion is calculated analogously by considering the addition of a neutralizing, positive unit charge, which does not interact with the charge $z_\mathrm{p} = -1$ at position x'.

Appendix B

In this appendix we present a correction to the expression for $\mathrm{pH} - \mathrm{p}K_0$, eq 27, derived in appendix A. For clarity, we will reserve n for the number of charges in the actual simulation and let m represent a general dissociation state.

It is clear from eqs 1, 27, and 28 that the result for a noninteracting system, i.e., $\Delta U_+ = \Delta U_- = 0$, is not $\Delta\mathrm{p}K = 0$ as it should be. Even for very long chains, a nonzero result is obtained if n is close to 1 or N. The reason is that the distribution of states is highly skewed (truncated at $m = 0$ and $m = N$) and we need to reevaluate $\mathrm{pH} - \mathrm{p}K_0$ if we want the value to correspond to the simulated $\alpha = n/N$. As a correction, we will embark on an iterative process where $\langle\alpha\rangle$ is estimated from eq 12, using a polynomial approximation for the electrostatic interactions

$$U'(\alpha) = \alpha^2 E'_2 + \alpha E'_1 \quad (29)$$

where E'_2 and E'_1 are constants to be determined from the simulation. With this approximation, we can express the weight of a dissociation state as

$$W'_m = e^{\beta\mu m}\binom{N}{m} e^{-\beta[(m/N)^2 E'_2 + (m/N)E'_1]} \quad (30)$$

where the binomial coefficient $\binom{N}{m}$ expresses the number of nonequivalent ways m identical charges can be put on N sites. Equating the calculated weight quotients $\ln(W_{n\pm1}/W_n)$ with the approximations $\ln(W'_{n\pm1}/W'_n)$, we get

$$\beta E'_1 = \frac{N}{2}[(2n+1)(\ln\sum_{x'=1}^{N}\langle e^{-\beta\Delta U_-(x',\boldsymbol{x}^n)}\rangle_n - \ln n) + (2n-1)(\ln\sum_{x'=1}^{N}\langle e^{-\beta\Delta U_+(x',\boldsymbol{x}^n)}\rangle_n - \ln(N-n))] \quad (31)$$

and

$$\beta E'_2 = -\frac{N^2}{2}[\ln\sum_{x'=1}^{N}\langle e^{-\beta\Delta U_-(x',\boldsymbol{x}^n)}\rangle_n - \ln\sum_{x'=1}^{N}\langle e^{-\beta\Delta U_+(x',\boldsymbol{x}^n)}\rangle_n - \ln(n(N-n))] \quad (32)$$

The iteration is initiated by calculating $\langle\alpha\rangle$ analogously to eq 12 using the weights given by eq 30 (with eqs 27, 31, and 32 for μ, E'_1, and E'_2, respectively)

$$\langle\alpha\rangle = \frac{\sum_{m=1}^{N} m e^{\beta\mu m}\binom{N}{m} e^{-\beta[(m/N)^2 E'_2 + (m/N)E'_1]}}{N\sum_{m=1}^{N} e^{\beta\mu m}\binom{N}{m} e^{-\beta[(m/N)^2 E'_2 + (m/N)E'_1]}} \quad (33)$$

If this value is not close enough to the simulated α

$$\Delta\mathrm{p}K = \mathrm{pH} - \mathrm{p}K_0 - \log\frac{\langle\alpha\rangle}{1-\langle\alpha\rangle} \quad (34)$$

is used to estimate a new value for $\mu = k_\mathrm{B}T\ln 10(\mathrm{pH} - \mathrm{p}K_0)$ (the initial value is given by eq 27) with the help of the simulated α, i.e.

$$\mathrm{pH} - \mathrm{p}K_0 = \Delta\mathrm{p}K + \log\frac{\alpha}{1-\alpha} \quad (35)$$

The new $\mathrm{pH} - \mathrm{p}K_0$ gives a new $\langle\alpha\rangle$, which, via a new $\Delta\mathrm{p}K$, gives an even better value for $\mathrm{pH} - \mathrm{p}K_0$ etc, as long as $\langle\alpha\rangle$ is not satisfactory. We used $|\langle\alpha\rangle - \alpha| < 0.0001$ as the convergence criterium.

Note that when $\Delta U_+ = \Delta U_- = 0$, $E'_1 = E'_2 = 0$ and the process of calculating $\langle\alpha\rangle$ leads to $\Delta pK = 0$, because $W_m = e^{\beta\mu m}\binom{N}{m}$ is the weight of dissociation state m for N noninteracting monomers (or monoacids).

The weakest link in the correction is the polynomial approximation. It neglects correlations and assumes that the chain conformations are fairly constant. An effective potential like the screened Coulomb potential would suggest only a quadratic term, $U'(\alpha) = \alpha^2 E'$, and equating $\ln(W_{n+1}/W_{n-1})$ with the corresponding approximation, we get

$$\beta E' = \frac{N^2}{4n}\left[\ln \sum_{x'=1}^{N} \langle e^{-\beta\Delta U_-(x',\boldsymbol{x}^n)}\rangle_n - \ln \sum_{x'=1}^{N} \langle e^{-\beta\Delta U_+(x',\boldsymbol{x}^n)}\rangle_n + \ln\frac{N-n}{n}\right] \quad (36)$$

This is enough to work as good approximation in many cases, but not at very low degrees of dissociation (about one or two charges on the chain), in particular at high salt concentrations. In this case, an inserted or removed charge can on average be far from other chain charges, which may allow the salt to almost completely screen its intramolecular interactions. At the same time, its interaction with its own ion atmosphere may be relatively large and negative. With just one term in the polynomial, $U'(\alpha)$ will be negative due to a negative E' and states with large n will be erroneously favored in the calculation of $\langle\alpha\rangle$. The weights for large n may even become so large that $\langle\alpha\rangle$ cannot converge to the simulated α. The linear term, $\alpha E'_1$, is thus needed to take into account the effects of the simple ions.

It is tempting to attribute the linear term to monomer−ion interactions and the quadratic term to intramolecular interactions, but that is an oversimplification, because the correlations and the conformational changes that are assumed to be negligible do play a roll and the two terms are mainly a device to fit an effective energy around a local dissociation state. For example, we know that the conformations change when α changes and for the approximation to work, the states where the conformations are appreciably different have to have a negligible weight.

We have indications that the approximation may eventually break down. In particular, for long, highly charged, chains at low salt concentrations E_2 can become negative. This prevented convergence for $N = 160$ with $\alpha \geq 0.8$, but it could be remedied by using only the quadratic term from eq 36. Despite its possible shortcomings, the mean field approximation does offer an improvement compared to eq 27 for $pH - pK_0$ when the total (finite chain) ΔpK is calculated. It is mainly needed at low and high degrees of dissociation. The fact that it may break down for very long chains is not serious, because the total ΔpK and the infinite-chain approximation are converging anyway and the calculation of the former becomes pointless.

References and Notes

(1) Christos, G. A.; Carnie, S. L. *J. Chem. Phys.* **1989**, *91*, 439.
(2) Christos, G. A.; Carnie, S. L. *J. Chem. Phys.* **1990**, *92*, 7661.
(3) Hooper, H. H.; Blanch, H. W.; Prausnitz, J. M. *Macromolecules* **1990**, *23*, 4820.
(4) Hooper, H. H.; Beltran, S.; Sassi, A. P.; Blanch, H. W.; Prausnitz, J. M. *J. Chem. Phys.* **1990**, *93*, 2715.
(5) Reed, C. E.; Reed, W. F. *J. Chem. Phys.* **1991**, *94*, 8479.
(6) Christos, G. A.; Carnie, S. L.; Creamer, T. P. *Macromolecules* **1992**, *25*, 1121.
(7) Barenbrug, T. M. A. O. M.; Smit, J. A. M.; Bedeaux, D. *Macromolecules* **1993**, *26*, 6864.
(8) Reed, C. E.; Reed, W. F. *J. Chem. Phys.* **1992**, *96*, 1609.
(9) Sassi, A. P.; Beltrán, S.; Hooper, H. H.; Blanch, H. W.; Prausnitz, J. M.; Siegel, R. A. *J. Chem. Phys.* **1992**, *97*, 8767.
(10) Ullner, M.; Jönsson, B.; Söderberg, B.; Peterson, C. *J. Chem. Phys.* **1996**, *104*, 3048.
(11) Ullner, M.; Jönsson, B. *Macromolecules* **1996**, *29*, 6645.
(12) Debye, P.; Hückel, E. *Phys. Z.* **1923**, *24*, 185.
(13) Valleau, J. P. *Chem. Phys.* **1989**, *129*, 163.
(14) Alfrey, T., Jr.; Berg, P. W.; Morawetz, H. *J. Polym. Sci.* **1951**, *7*, 543.
(15) Fuoss, R. M.; Katchalsky, A.; Lifson, S. *Proc. Natl. Acad. Sci. U.S.A.* **1951**, *37*, 579.
(16) Marcus, R. A. *J. Chem. Phys.* **1955**, *23*, 1057.
(17) Wennerström, H.; Jönsson, B.; Linse, P. *J. Chem. Phys.* **1982**, *76*, 4665.
(18) Verwey, E. J. W.; Overbeek, J. T. G. *Theory of the Stability of Lyophobic Colloids*; Elsevier: Amsterdam, 1948.
(19) Beresford-Smith, B. Some Aspects of Strongly Interacting Colloidal Dispersions. Ph.D. Thesis, Australian National University: Canberra, 1985.
(20) Linse, P.; Jönsson, B. *J. Chem. Phys.* **1983**, *78*, 3167.
(21) Jönsson, B.; Ullner, M.; Peterson, C.; Sommelius, O.; Söderberg, B. *J. Phys. Chem.* **1996**, *100*, 409.
(22) Kesvatera, T.; Jönsson, B.; Thulin, E.; Linse, S. *J. Mol. Biol.* **1996**, *259*, 828.
(23) Widom, B. *J. Chem. Phys.* **1963**, *39*, 2808.
(24) Svensson, B.; Woodward, C. E. *Mol. Phys.* **1988**, *64*, 247.
(25) Metropolis, N. A.; Rosenbluth, A. W.; Rosenbluth, M. N.; Teller, A.; Teller, E. *J. Chem. Phys.* **1953**, *21*, 1087.
(26) Ullner, M.; Staikos, G.; Theodorou, D. N. *Macromolecules* **1998**, *31*, 7921.
(27) Manning, G. S. *J. Chem. Phys.* **1969**, *51*, 924.
(28) Mandel, M. *Eur. Polym. J.* **1970**, *6*, 807.
(29) Kawaguchi, Y.; Nagasawa, M. *J. Phys. Chem.* **1969**, *73*, 4382.
(30) Ullner, M.; Jönsson, B.; Peterson, C.; Sommelius, O.; Söderberg, B. *J. Chem. Phys.* **1997**, *107*, 1279.
(31) Press, W. P.; Flannery, B. P.; Teukolsky, S. A.; Vettering, W. T. *Numerical Recipes, The Art of Scientific Computing*; Cambridge University Press: Cambridge, England, 1986.
(32) Olander, D. S.; Holtzer, A. *J. Am. Chem. Soc.* **1968**, *90*, 4549.
(33) Muroga, Y.; Suzuki, K.; Kawaguchi, Y.; Nagasawa, M. *Biopolymers* **1972**, *11*, 137.

MA991056K